Plasma-Induced Damage and Recovery on Au/n-GaN Schottky Diode in Different Processes

Japanese Journal of Applied Physics **51** (2012) 076503 **REGULAR PAPER**
DOI: 10.1143/JJAP.51.076503

Plasma-Induced Damage and Recovery on Au/n-GaN Schottky Diode in Different Processes

ChangYong Lee*, Hiroto Sekiguchi, Hiroshi Okada[1], and Akihiro Wakahara

Department of Electrical and Electronic Information Engineering, Toyohashi University of Technology, Toyohashi, Aichi 441-8580, Japan
[1] *Electronics-Inspired Interdisciplinary Research Institute (EIIRIS), Toyohashi University of Technology, Toyohashi, Aichi 441-8580, Japan*

Received March 12, 2012; accepted May 1, 2012; published online June 26, 2012

The effects of plasma-induced damage on deep traps in n-GaN have been investigated using current–voltage (*I*–*V*), capacitance–voltage (*C*–*V*), and photocapacitance (PHCAP) measurements. The Au/n-GaN Schottky barrier diodes were fabricated in an inductively coupled plasma ion etching (ICP-RIE) system. After mesa etching to achieve ohmic contact, the n-GaN surface, at which Schottky contacts are fabricated, is etched ~100 nm by ICP-RIE with various Cl_2/Ar ratios and RIE bias powers (P_B), to introduce plasma damage. The electrical properties of the fabricated Shottky barrier diodes (SBDs) strongly dependent on the RIE gas composition and the bias power P_B applied to the sample stage. In order to overcome the residue and plasma damage on the Schottky area, the samples were treated with HCl at 110 °C for 30 min. Several deep levels (1.8, 2.5, and 3.0 eV below the conduction band) were detected by PHCAP measurement. Improved electrical characteristics were achieved as a result of the HCl treatment and sintering process. The PHCAP measurement results also revealed the effectiveness of thermal and chemical treatments.

1. Introduction

Currently, the emergent interest in ultraviolet (UV) devices for scientific instruments has produced research efforts on wide-band-gap materials. With its wide direct band gap, high-saturation velocity and high thermal conductivity, GaN is one of the attractive compound semiconductors for use in optoelectronic and microelectronic device applications. Such materials and their ternary and quaternary alloys cover the deep- to mid-UV radiation range for devices such as light-emitting diodes (LEDs), laser diodes (LDs), and UV detectors.[1–5] However, the high bond strength of GaN also presents some difficulties for device applications. Device fabrication processes for GaN-based materials usually rely on dry etching methods that require a variety of plasma and ion conditions known to lead to surface damage.[6–8] Moreover, the dry etching process induces ion-induced lattice defects, discharge-gas-related residues and non-stoichiometric surfaces, which lead to the degradation of device characteristics, such as the electrical and optical device properties.[9–12] In order to detect and identify these defects in GaN-based materials, various characterization techniques, such as photoluminescence (PL), cathodeluminescence (CL), deep-level transient spectroscopy (DLTS), and photocapacitance (PHCAP) methods, have been employed.[13–21] The most perceptive DLTS spectroscopy is yet to be fully invented for the characterization of electronic fields in semiconductors. There is a limitation in the use of DLTS to wide-band-gap semiconductors because of the much higher activation energy for trapped charges compared with the thermal energy. The accessible range of band-gap energies is restricted to within ~0.9 eV of any band edge for typical trap parameters and practical measurement conditions owing to the thermal energy of charge emission. The electrical and physical properties of various deep-level defects existing in the GaN-based materials still remain uncertain. However, few investigations of deep levels, particularly at the plasma-induced damage in GaN, have been reported. In this work, we characterize the Schottky diodes fabricated on GaN surfaces etched by inductively coupled plasma ion etching (ICP-RIE). Current–voltage (*I*–*V*), capacitance–voltage (*C*–*V*), and PHCAP measurements were used to access deep levels throughout the band gap. Also, wet treatments have been examined for overcoming the plasma-induced damage.

*E-mail address: cylee@int.ee.tut.ac.jp

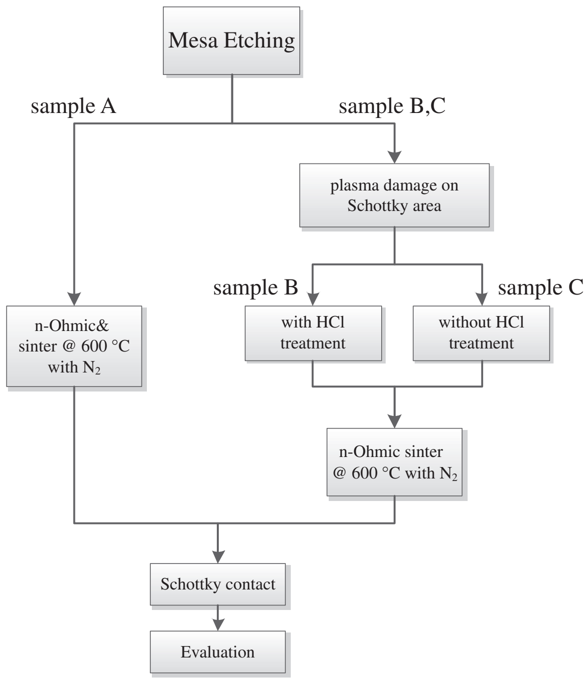

Fig. 1. Complete process of the Au/n-GaN Schottky diode with plasma-induced damage layer structure.

2. Device Structure and Fabrication Process

The process flow and schematic image of the fabricated Au/n-GaN Schottky diode are shown in Figs. 1 and 2. There are three different process paths: samples A (nontreated), B (ICP-treated), and C (ICP + HCl treated). Si-doped n-GaN/n^+-GaN epitaxial wafers with the donor concentrations of 2.5×10^{17} and 5×10^{18} cm^{-3} were used for all fabricated SBDs. The n-GaN layer was etched 600 nm using ICP-RIE with 120 W antenna power (P_A) and 30 W bias power (P_B) to access the n^+-GaN layer as the ohmic contact. The $Cl_2/Ar = 30/10$ sccm mixture was employed as an etching gas. After mesa etching, the n-GaN (~100 nm) layer was exposed to Cl_2/Ar plasma in the ICP-RIE apparatus at various bias powers and Cl_2/Ar ratios, where the Cl_2/Ar

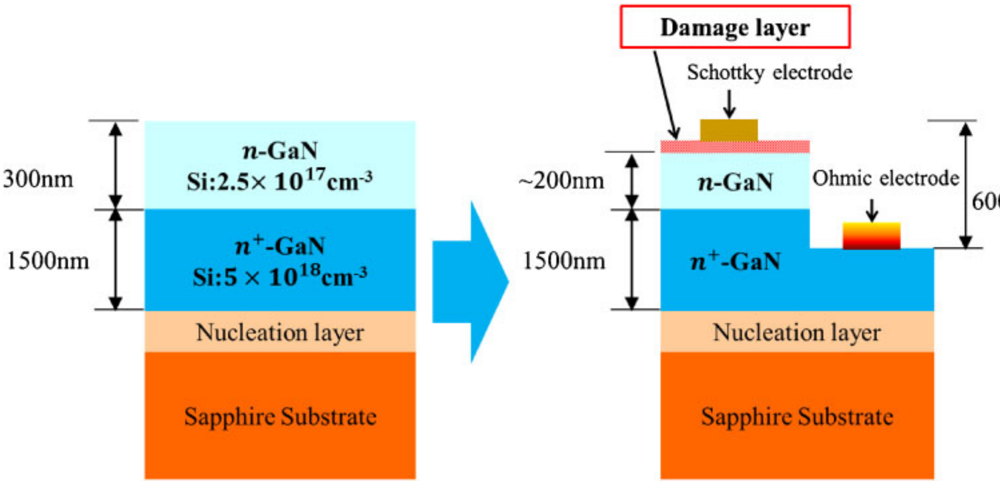

Fig. 2. (Color online) Schematic diagram of the Au/n-GaN Schottky diode with plasma-induced damage layer structure.

ratio was varied under a constant total amount of $Cl_2 + Ar =$ 40 sccm, and bias power P_B was applied to the sample stage to estimate plasma-induced damage underneath the Schottky contact area, as shown in Fig. 1. In order to clarify the effect of wet etching on the plasma-induced damage, the samples were treated with HCl at 110 °C for 30 min before fabricating the ohmic electrode. Ti/Al/Ti/Au (30/30/20/200 nm) was deposited on the n^+-GaN layer by electron beam (EB) evaporation as the ohmic electrode. Rapid thermal annealing (RTA) was used for alloying the ohmic contact at 600 °C for 3 min under N_2 ambient. Finally, a 200-nm-thick Au Schottky electrode was formed on the plasma-exposed surface.

The *I–V* characteristics were measured with a Keithley 4200 semiconductor parameter analyzer, and *C–V* and PHCAP data were measured using an Agilent 4284A precision LCR meter. PHCAP measurements were performed using a quiescent bias of −3 V followed by a 10 s filling pulse to 1 V in the dark. After a 20 s settling time in the dark to allow thermal transients to complete, the PHCAP was measured for 600 s under illumination photon energy from 1.2 to 3.0 eV, using monochromated light from a Xe lamp (Ushio Optical ModuleX) filtered with a 0.25 m monochromator.

3. Results and Discussion

Figure 3 shows the *I–V* characteristics of SBDs treated by the process described above. It is clearly seen that leakage current density increased as the bias power for ICP-RIE was increased. The Schottky barrier height (SBH) estimated from the *I–V* characteristics was also reduced from 1.04 eV for SBD without plasma exposure (sample A) to 0.71 eV ($P_B = 30$ W), 0.67 eV ($P_B = 60$ W), and 0.62 ($P_B = 100$ W), as the bias power was increased. The leakage current density increased more than five orders of magnitude after plasma exposure with the bias power of $P_B = 100$ W compared with that of the unexposed sample. The leakage current density was also strongly dependent on the gas composition during the ICP-RIE process, i.e., the minimum leakage current density was obtained at the Ar composition of 25%, as shown in Fig. 3. The ionized donor concentration (N_d) estimated from the *C–V* measurement is illustrated in

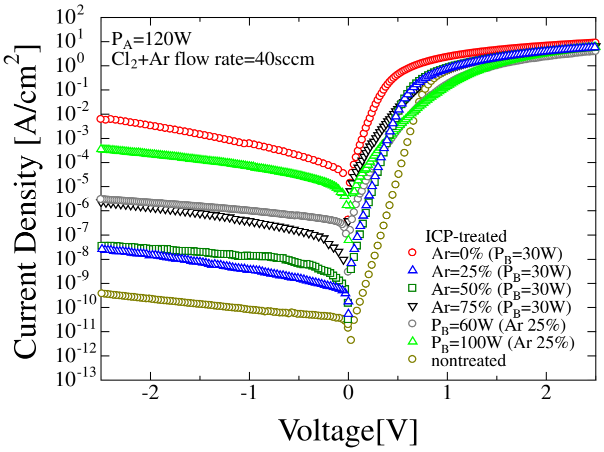

Fig. 3. (Color online) *I–V* characteristics of Schottky diodes with various bias powers (P_B) and Cl_2/Ar gas ratios.

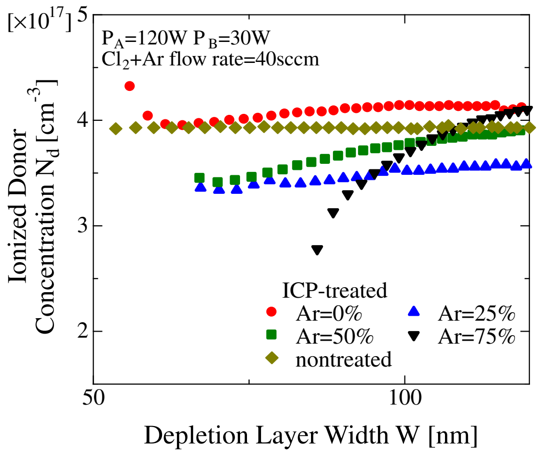

Fig. 4. (Color online) Calculated value of ionized donor concentration versus depth from the surface determined by *C–V* measurement.

Fig. 4. When the RIE is carried out without Ar, N_d seems to increase within 70 nm from the surface. However, N_d decreases upon increasing the Ar concentration. When the RIE process was carried out in Ar concentration higher than

75%, the N_d-decreased region was as deep as 120 nm from the surface. These results suggest that Ar ions produce deep traps while Cl_2 plasma induces shallow donorlike defects.[6] Generally, plasma etching is carried out by both ion bombardment and the chemical reaction between the GaN surface and reactive species in the plasma. In the case of Ar-containing plasma etching, Ar^+ ions are accelerated by the electric field generated in the plasma sheath and the accelerated ions sputtering the atoms, which is located at/near the surface. Through this process, some atoms move from the lattice site, and thus lattice defects, such as interstitials, antisites, and vacancies, are generated. The electric field in the sheath becomes strong as the bias power increases, and the energy of Ar^+ ions also becomes high, and thus, the number of defects introduced increases with the increase in the energy of the ions, i.e., bias power P_B. In contrast, in the case of activated chloride, either neutral or ionized atoms and/or excited molecules react with both Ga and N atoms at the surface and create $GaCl_x$ and NCl_x as the reactant. Desorption of these reactants is enhanced by the occurrence of physical sputtering. Su *et al.* reported residues of $GaCl_x$ and NCl_x species on the GaN surface after Cl_2-based RIE,[22] and Nakamura *et al.* reported intrinsic defects due to a deficiency of nitrogen in their Ar-plasma-treated GaN.[23] Because of the different electronegativities in polar nitrides, normally, the GaN(0001) surface is positively charged. However, upon the adsorption of the chlorinated species on the GaN surface, it becomes negatively charged. In addition, the Cl easily reacts with GaN, and the vaporization of NCl_3 is higher than $GaCl_3$, then, the number of nitrogen vacancies (V_N), which act as electron donors, increases at the near-surface region. As a result, the negatively charged surface decreases the SBH and the V_N increases ionized donor concentration.[22,24,25)]

In order to reduce the plasma damage on the device performance, the effects of the wet treatment of the etched surface on the device properties were investigated. Figure 5(a) shows I–V characteristics of the SBDs with different surface treatments before forming the Schottky contact. The HCl-treated samples show sufficient improvement of the reverse bias leakage current level. The recovery of etch-induced damage is of great importance in the fabrication of GaN devices. The leakage current density was found to decrease more than two orders compared with the untreated samples. This result suggests that Cl_2-plasma-induced shallow-donor-like defects could be removed by treatment with boiled HCl. Deep traps could be annealed out by sintering.[26] In order to examine the deep trap, time-dependent current (I–t) characteristic measurement was carried out, as shown Fig. 5(b). After the initialization process at -5 V for 2 min, deep levels were filled by forward bias at $+1$ V for 30 s, then the current under reverse bias of -1 V, was measured. Although the leakage current level for the HCl-treated sample was almost the same as that of the nontreated SBD, the discharge transient current due to the emission of captured electrons from deep traps was still observed.

The effects of etch-induced damage and its recovery on the Schottky area were further investigated using PHCAP measurements. In this study, the photocapacitance signal is defined as ΔC_{ss}. Here, C_0 is the diode capacitance under the

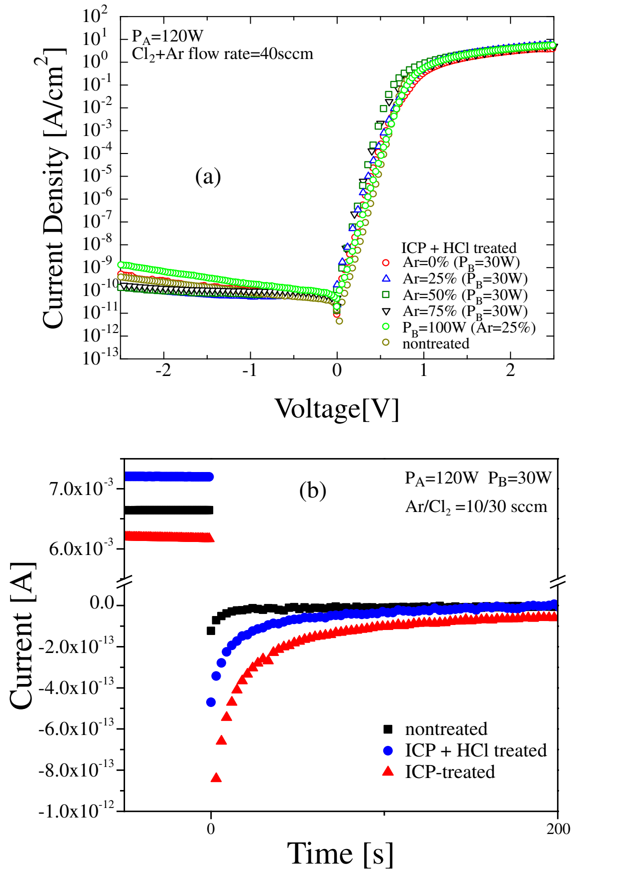

Fig. 5. (Color online) (a) I–V characteristics after HCl treatment, and (b) time-dependent current characteristics of samples nontreated, and before and after HCl treatment, measured at -1 V bias after initialization process at -5 V for 2 min; deep levels were filled by applying $+1$ V for 30 s.

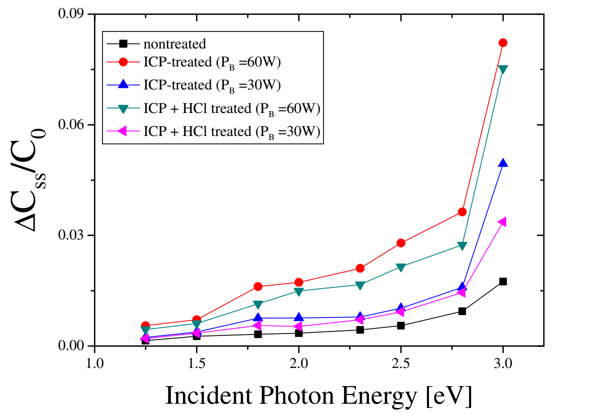

Fig. 6. (Color online) Steady-state photocapacitance spectra versus photon incident energy from the Au/n-GaN Schottky samples nontreated, with 30 and 60 W of RIE bias power, and with and without HCl treatment, measured at 300 K with 600 s illumination.

reverse-biased condition in the dark before optical excitation, and ΔC_{ss} is the change in the steady-state photocapacitance owing to illumination. Figure 6 shows the capacitance change as a function of photon energy at a quiescent bias of -3 V, and the steady-state photocapacitance spectra of the Schottky samples at $T = 300$ K. For low trap densities (i.e., $N_T \ll N_D$), the changes in ΔC_{ss} are proportional to the density of the corresponding deep level.[27] We can observe photoemissions at ~1.8, ~2.5, and ~3.0 eV below the conduction band. Similar photocapacitance spectra results have been reported by Hierro *et al.* for their deep levels in n-GaN Schottky diodes.[28] The range of 1.5–2.5 eV is attributed to the gallium vacancy (V_{Ga}) or a complex between V_{Ga} and donor impurities.[29–32] This state is correlated with the well-known yellow luminescence (YL) band observed for n-GaN.[33,34] The ~3.0 eV level is correlated to residual acceptors other than Mg in the n-GaN Schottky diode.[35] The results of our measurements reveal that the bombarding ions induced deep-level defects and the induced damage is proportional to RIE bias power, as shown in Fig. 6. It is also observed that deep-level induced damage was reduced after the HCl treatment.

4. Conclusions

The effects of plasma-induced damage were investigated using Au/n-GaN SBDs with various bias powers and Cl_2/Ar ratios in the ICP etching process. As the plasma bias power increased, the SBH decreased and reverse bias leak current density increased. Also, electrical properties strongly depended on the Cl_2/Ar ratio. The HCl treatment and sintering process on the etched GaN surface improved the PHCAP characteristics and decreased the specific deep-level traps. The HCl treatment and sintering process effectively recovered the plasma-induced damage on GaN surfaces. However, the discharge transient current due to the emission of captured electrons at deep traps was still observed.

Acknowledgements

This work is supported in part by the International Program of Regional Innovation Cluster Program "Tokai Region Nanotechnology Manufacturing Cluster" and the Global COE Program "Frontiers of Intelligent Sensing" of the Ministry of Education, Culture, Sports, Science and Technology of Japan (MEXT). Parts of the experiments, particularly device fabrication processing, were carried out at the LSI facilities in EIIRIS, Toyohashi Tech.

1) S. Nakamura, T. Mukai, and M. Senoh: Jpn. J. Appl. Phys. **30** (1991) L1998.
2) T. J. Prosa, P. H. Clifton, H. Zhong, A. Tyagi, R. Shivaraman, S. P. DenBaars, S. Nakamura, and J. S. Speck: Appl. Phys. Lett. **98** (2011) 191903.
3) R. G. Banal, R. G. Banal, M. Funato, and Y. Kawakami: Appl. Phys. Lett. **99** (2011) 011902.
4) C. Y. Lee, F. Matsuno, Y. Hashimoto, H. Okada, K. Sawada, and A. Wakahara: Jpn. J. Appl. Phys. **51** (2012) 044101.
5) J. Zhang, H. Zhao, and N. Tansu: Appl. Phys. Lett. **98** (2011) 171111.
6) M. Nakaji, T. Egawa, H. Ishikawa, S. Arulkumaran, and T. Jimbo: Jpn. J. Appl. Phys. **41** (2002) 493.
7) J. Y. Chen, C. J. Pan, and G. C. Chi: Solid-State Electron. **43** (1999) 649.
8) R. Qiu, H. Liu, D. Chen, R. Zhang, and Y. Zheng: Appl. Surf. Sci. **257** (2011) 2700.
9) H. K. Cho, F. A. Khan, I. Adesida, Z.-Q. Fang, and D. C. Look: J. Phys. D **41** (2008) 155314.
10) T. Hashizume and H. Hasegawa: Appl. Surf. Sci. **234** (2004) 387.
11) A. Koudymov, M. S. Shur, and G. Simin: IEEE Electron Device Lett. **28** (2007) 332.
12) J. M. Lee, K. M. Chang, S. W. Kim, C. Huh, I. H. Lee, and S. J. Park: J. Appl. Phys. **87** (2000) 7667.
13) Y. S. Park, C. J. Park, C. M. Park, J. H. Na, J. S. Oh, I. T. Yoon, H. Y. Cho, T. W. Kang, and J.-E. Oh: Appl. Phys. Lett. **86** (2005) 152109.
14) N. Nepal, M. L. Nakarmi, J. Y. Lin, and H. X. Jiang: Appl. Phys. Lett. **89** (2006) 092107.
15) D. Y. Protasov, O. E. Tereshchenko, K. S. Zhuravlev, A. Y. Polyakov, N. B. Smirnov, and A. V. Govorkov: Physica B **404** (2009) 4870.
16) Z. Zhang, C. A. Hurni, A. R. Arehart, J. Yang, R. C. Myers, J. S. Speck, and S. A. Ringel: Appl. Phys. Lett. **100** (2012) 052114.
17) A. R. Arehart, A. A. Allerman, and S. A. Ringel: J. Appl. Phys. **109** (2011) 114506.
18) Z.-Q. Fang, D. C. Look, D. H. Kim, and I. Adesida: Appl. Phys. Lett. **87** (2005) 182115.
19) P. Hacke and H. Okushi: Appl. Phys. Lett. **71** (1997) 524.
20) A. Hierro, S. A. Ringel, M. Hansen, J. S. Speck, U. K. Mishra, and S. P. DenBaars: Appl. Phys. Lett. **77** (2000) 1499.
21) M. A. Py, Ch. Zellweger, V. Wagner, J.-F. Carlin, H.-J. Buehlmann, and M. Ilegems: Phys. Status Solidi A **202** (2005) 572.
22) S.-H. Su, C.-C. Hou, M.-H. Lin, M. Yokoyama, S.-M. Chen, and H. Kuan: Jpn. J. Appl. Phys. **46** (2007) 965.
23) S. Nakamura, M. Suda, M. Suhara, and T. Okumura: CS Mantech Conf., 2006, p. 275.
24) H.-W. Jang, J.-H. Lee, and J.-L. Lee: Appl. Phys. Lett. **80** (2002) 3955.
25) S. J. Pearton, C. R. Abernathy, and F. Ren: *Gallium Nitride Processing for Electronics, Sensors and Spintronics* (Springer, Heidelberg, 2006) p. 104.
26) V. R. Reddy, M. S. Reddy, and P. K. Rao: Microelectron. Eng. **87** (2010) 117.
27) W. Götz, N. M. Johnson, R. A. Street, H. Amano, and I. Akasaki: Appl. Phys. Lett. **66** (1995) 1340.
28) A. Hierro, D. Kwon, S. A. Ringel, M. Hansen, J. S. Speck, U. K. Mishra, and S. P. DenBaars: Appl. Phys. Lett. **76** (2000) 3064.
29) T. Ogino and M. Aoki: Jpn. J. Appl. Phys. **35** (1980) 74.
30) J. Neugebauer and C. G. Van de Walle: Appl. Phys. Lett. **69** (1996) 503.
31) U. Kaufmann, M. Kunzer, H. Obloh, M. Maier, Ch. Manz, A. Ramakrishnan, and B. Stantic: Phys. Rev. B **59** (1999) 5561.
32) X. Zhang, P. Kung, A. Saxler, D. Walker, T. C. Wang, and M. Razeghi: Appl. Phys. Lett. **67** (1995) 1745.
33) A. Armstrong, A. R. Arehart, D. Green, U. K. Mishra, J. S. Speck, and S. A. Ringel: J. Appl. Phys. **98** (2005) 053704.
34) P. Hacke, H. Okushi, T. Kuroda, T. Detchprohm, K. Hiramatsu, and N. Sawaki: J. Cryst. Growth **189** (1998) 541.
35) G. Yi and B. W. Wessels: Appl. Phys. Lett. **68** (1996) 3769.